Paper
Int'l J. of Aeronautical & Space Sci. 18(2), 290–299 (2017)
DOI: doi.org/10.5139/IJASS.2017.18.2.290

IJASS
International Journal of Aeronautical and Space Sciences

Reconfigurable Flight Control Design for the Complex Damaged Blended Wing Body Aircraft

Jongmin Ahn*

Agency for Defense Development, Daejeon 34186, Republic of Korea

Kijoon Kim, Seungkeun Kim***, and Jinyoung Suk******

Chungnam National University, Daejeon 34134, Republic of Korea

Abstract

Reconfigurable flight control using various kinds of adaptive control methods has been studied since the 1970s to enhance the survivability of aircraft in case of severe in-flight failure. Early studies were mainly focused on the failure of actuators. Recently, studies of reconfigurable flight controls that can accommodate complex damage (partial wing and tail loss) in conventional aircraft were reported. However, the partial wing loss effects on the aerodynamics of conventional type aircraft are quite different to those of BWB(blended wing body) aircraft. In this paper, a reconfigurable flight control algorithm was designed using a direct model reference adaptive method to overcome the instability caused by a complex damage of a BWB aircraft. A model reference adaptive control was incorporated into the inner loop rate control system enhancing the performance of the baseline control to cope with abrupt loss of stability. Gains of the model reference adaptive control were polled out using the Liapunov's stability theorem. Outer loop attitude autopilot was designed to manage roll and pitch of the BWB UAV as well. A 6-DOF dynamic model was built-up, where the normal flight can be made to switch to the damaged state abruptly reflecting the possible real flight situation. 22% of right wing loss as well as 25% loss for both vertical tail and rudder control surface were considered in this study. Static aerodynamic coefficients were obtained via wind tunnel test. Numerical simulations were conducted to demonstrate the performance of the reconfigurable flight control system.

Key words: MRAC, Direct Adaptive Control, BWB UAV, Complex Damaged Aircraft

1. Introduction

Classical PID control has demonstrated its robustness and effectiveness through countless applications in various kinds of aircraft. However it has a weak point in that it can't adapt to drastic changes in the flight dynamics of the aircraft due to actuator failure or the configuration change of the aircraft like the partial loss of a wing or tail. The performance of PID control deteriorates under these severe changes in flight characteristics, sometimes resulting in the loss of control and stability.

The safe landing of an Israeli Air Force F-15 after the loss of its right wing invoked research in reconfigurable flight control systems in 1983. Self-Repairing Flight Control System(1984~1990, NASA) and the RESTORE project are representative research projects of the reconfigurable flight control system. The Self-Repairing Flight Control System project assumed the conditions that the control surface lock failed and the right horizontal tail was missed. NASA's F-15 research aircraft was used for flight test from 1989 to 1990 [1]. The right horizontal tail missing condition was simulated by the combination of control surfaces' deflection. A different approach using neural net adaptive control was designed to cope with the control surface failure or damage in the RESTORE project [2-4]. The reconfigurable flight control system was tested using the X-36 unmanned air vehicle in

* Principal Research Engineer
** Ph. D Student
*** Associate Professor
**** Professor Corresponding author: jsuk@cnu.ac.kr

Received: April 6, 2016 Revised: February 25, 2017 Accepted: April 6, 2017

http://ijass.org pISSN: 2093-274x eISSN: 2093-2480

December 1998 [5].

By the 2000s, the focus of reconfigurable flight control system research has switched from actuator malfunction to complex damage. In 2006, the hybrid direct-indirect neural net adaptive control method was designed and reconfiguration performance was tested in a medium-fidelity simulation environment of the partial wing loss of the Generic Transport Model [6]. Damien B. Jordan introduced damage tolerant control in 2010. The automatic supervisory adaptive controller was designed to recover from structural failures and an automatic upset recovery algorithm was included in the attitude autopilot. The inner-loop controllers were composed of baseline controllers and model reference adaptive control to recover the degraded control performance of the baseline controllers. The controllers were implemented on a scaled unmanned variant of an F-18 and the controller was demonstrated through flight tests in April 2008. The damage on the right wing, a 60% loss of the area moment, was tested successfully [7]. In 2013, a damage tolerant adaptive control for BWB aircraft was introduced. In this research, a neural net adaptive controller was designed to compensate for the baseline controller, and the performance was demonstrated by causing a partial loss of the left wing's area moment(33%) during the flight test [8].

L1 adaptive control Theory was introduced in 2000's and many researches of reconfigurable/damage adaptive flight control using L1 adaptive controller were also reported [9-12].

This paper contains a reconfigurable control design capable of adapting to complex damage incurred on a BWB UAV. The attitude autopilot and rate command following controller was designed as the baseline controller. The model reference adaptive controller was designed to restore the control power after the complex damage on both the UAV's right wing and vertical tail. The 6-DOF model of the test UAV was developed using data collected from wind tunnel tests. The complex damage was modeled to reflect a loss in the area moment of 22% and 25% for the right wing and vertical tail(including rudder) respectively. Numerical simulations were conducted to show the baseline controller's degradation in performance after the damage. Also, the performance of the model reference adaptive controller was demonstrated.

This paper consists of 5 sections. In the 1'st section, general history of the reconfigurable flight control design was introduced, and then modeling of the 6-DOF of BWB test UAV for the complex damaged state as well as normal state are described in the 2'nd section. The 3'rd section, which is main part of this paper, contains the structure of the reconfigurable controller and design of the each control loop. In the section 4, the nonlinear simulation result, which shows the effects of the complex damage on the baseline controller and the MRAC's capability to cope with the damage, is presented. The final section contains the summary of the result of this study.

2. Aircraft Dynamics and Complex Damage Modeling

The basic specification of the BWB research UAV, which is applied in this study, is summarized in Table 1.

Figure 1 shows the shape and dimension of the BWB research UAV. The normal configuration has good short period damping and marginally stable dutch-roll mode at the control law design point(100m altitude and 30 m/sec airspeed) as indicated in the fig. 3 and 4.

To simulate the complex damage condition of the BWB UAV, wind tunnel tests were performed for the 8 different

Table 1. Specification of the aircraft

Parameter	Value	Units
Mass	12.003	kg
Wing Area	1.561	m^2
Wing Span	1.98	m

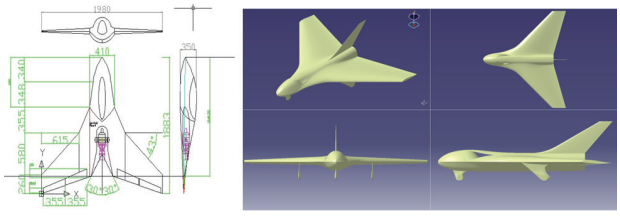

Fig. 1. Specification of the BWB UAV

Table 2. Model Configurations for Wind Tunnel Test

		Right Wing			
		No Damage	22% damage	60% damage	78.4% damage
Vertical Tail	No damage	Config. 1	Config. 3	Config 5	Config 7
	100% damage	Config. 2	Config. 4	Config 6	Config 8

configurations shown in Table 2.

To estimate the aerodynamic data of complex damage (22% wing loss and 25% loss of vertical tail and rudder), the data collected from the wind tunnel test were interpolated under the assumption that the aerodynamic coefficients vary linearly between Configuration 3 and Configuration 4 in table2. The reference [13] contains the wind tunnel test data for each damage configuration.

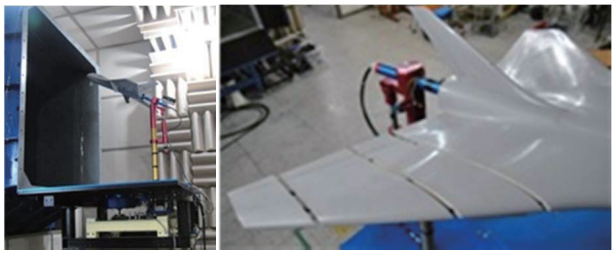

Fig. 2.Wind Tunnel Test

The change of the dynamic stability derivatives like C_{l_p} and C_{n_r} was also considered. It was assumed that the dynamic stability derivatives shall be decreased as same proportion of the moment area decrease.

The change of mass and center of gravity due to complex damage was calculated using CATIA function of inertia measurement. In this calculation, it was considered that the material properties are uniform and the change of the center of gravity in z-axis direction due to the partial loss of vertical tail can be neglected. Table 3 and 4 show the mass property and configuration change due to complex damage [13].

2.1 Force and Moment Equation

Aircrafts are generally assumed to be symmetric and have a C.G. located on the x-z plane in the body axis system which lead to the derivation of simple force and moment equations. However, once complex damage is taken into

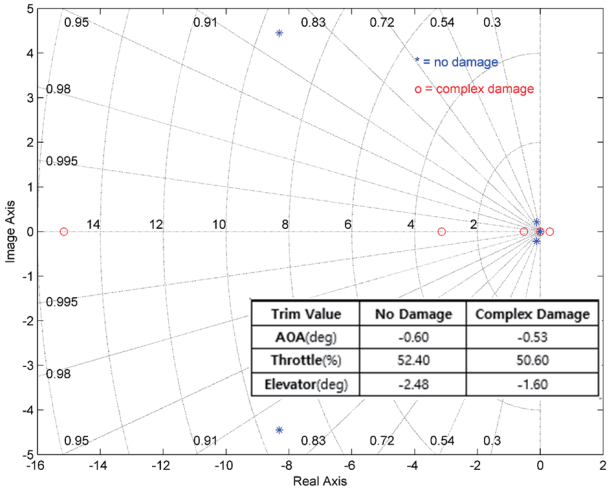

Fig. 3. Poles of Longitudinal Flight Mode

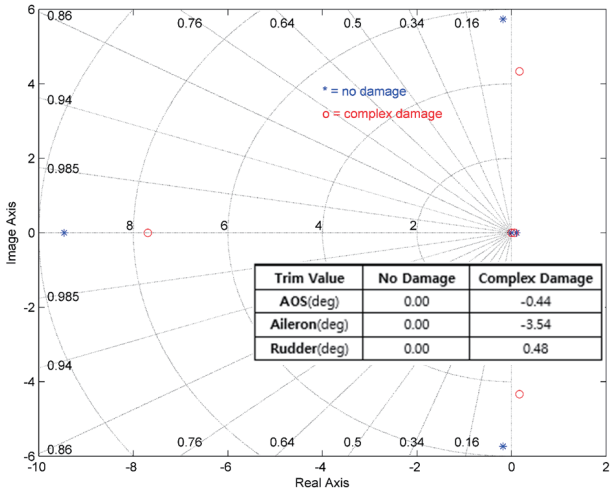

Fig. 4. Poles of Lateral Directional Flight Mode

Table 3. Mass Property Change Due to Complex Damage

Moment of Inertia ($kg \cdot m^2$)	Damage Condition		Variation Due to Damage (%)	
	No Damage	Complex Damage		
I_xx	1.527	1.416	7.3	
I_yy	1.733	1.699	2.0	2.0
I_zz	3.207	3.062	4.5	4.5
I_xy	0	0.06	-	-
I_xz	-0.015	-0.015	0.0	0.0
I_yx	0	0.06	-	-
I_yz	0	-0.00038	-	-
I_zx	-0.015	-0.015	0.0	0.0
I_zy	0	-0.00038	-	-

DOI: doi.org/10.5139/IJASS.2017.18.2.290

consideration, these assumptions are no longer valid. In this paper, the following force and moment equations were applied to simulate the flight dynamics of the damaged aircraft.

$$X = m(\dot{u} + \dot{q}\Delta z - \dot{r}\Delta y - rv + qw + g\sin\theta) \quad (1)$$

$$Y = m(\dot{v} - \dot{p}\Delta z + \dot{r}\Delta x + ru - pw - g\cos\theta\sin\emptyset) \quad (2)$$

$$Z = m(\dot{w} + \dot{p}\Delta y - \dot{q}\Delta x - qu + pv - g\cos\theta\cos\emptyset) \quad (3)$$

$$L = I_{xx}\dot{p} - I_{xy}\dot{q} - I_{xz}\dot{r} + I_{xy}pr - I_{xz}pq + (I_{xx} - I_{yy})qr + I_{yz}(r^2 - q^2) + m(qv + rw)\Delta x + m(\dot{w} - qu)\Delta y - m(\dot{v} - ru)\Delta z \quad (4)$$

$$M = -I_{xy}\dot{p} + I_{yy}\dot{q} - I_{yz}\dot{r} + I_{yz}pq - I_{xy}qr + (I_{xx} - I_{zz})pr + I_{xz}(p^2 - r^2) - m(\dot{w} - pv)\Delta x + m(pu + rw)\Delta y + m(\dot{u} - rv)\Delta z \quad (5)$$

$$N = -I_{xz}\dot{p} - I_{yz}\dot{q} + I_{zz}\dot{r} + I_{xz}qr - I_{yz}pr + (I_{yy} - I_{xx})pq + I_{xy}(q^2 - p^2) + m(\dot{v} - pw)\Delta x - m(\dot{u} + qw)\Delta y + m(pu + qv)\Delta z \quad (6)$$

In equations (1)~(6), Δx, Δy, Δz correspond to the variation of the C.G. caused by damage.

2.2 The Change of the Aircraft Dynamics Due to Complex Damage

In case of the complex damage of the conventional type aircraft, the effects of the damage have a tendancy to affect independently. For example, the partial wing loss affects on roll mode, the partial loss of the vertical tail affects on dutch roll mode, and so on. The cross effects are negligible. However, it was reported that the partial wing loss of an BWB aircraft decreases the lift coefficient(C_{L_α}) and short period natural frequency(C_{m_α}) as well as roll mode frequency in 2011 [14]. The partial loss of vertical tail decreases the directional stability(C_{n_β}) and it cause unstable dutch roll mode. Figs. 3 and 4 shows the movement of the poles and the change of the trim values due to the complex damage of the BWB UAV for the same trim condition(True Air Speed : 30 m/sec, Altitude : 100 m, Wing Level Trim). The conjugate short period poles moved to the real axis due to the damage and it shows that it is nearly neutral state of longitudinal static stability. In case of the poles of roll mode also moved toward the origin and the movement of poles of dutch roll mode corresponds to the what we expected from the reference [14].

The movement of poles shows the modeling of the complex damage is adequate to evaluate the performance of the reconfigurable flight controller. The linear time invariant state space model of the BWB UAV is as follows.

$$\dot{x} = Ax + Bu$$

$$y = Cx + Du \qquad (C = I_3,\ D = 0)$$

Where the longitudinal, lateral-directional state variables and control inputs are defined as follows.

$$x_{LON} = [V_t\ \alpha\ q\ \theta\ h]',\quad u_{LON} = [\delta_{thr}\ \delta_e]'$$

$$x_{LAT} = [\beta\ p\ r\ \phi\ \psi]',\quad u_{LAT} = [\delta_a\ \delta_r]'$$

The following linear matrixes shows the change of the flight dynamics caused by the complex damage.

$$\text{A\_LON} = \begin{bmatrix} -0.3426 & -34.8923 & 0.0000 & -9.8060 & 0.0000 \\ -0.0219 & -6.1916 & 0.9513 & 0.0000 & 0.0000 \\ 0.0000 & -25.2710 & -10.3117 & 0.0000 & 0.0000 \\ 0.0000 & 0.0000 & 1.0000 & 0.0000 & 0.0000 \\ 0.0000 & 30.0000 & 0.0000 & -30.0000 & 0.0000 \end{bmatrix}$$

$$\text{B\_LON} = \begin{bmatrix} 9.8070 & -3.1166 \\ 0.0033 & -2.4412 \\ 0.0000 & -150.6280 \\ 0.0000 & 0.0000 \\ 0.0000 & 0.0000 \end{bmatrix}$$

$$\text{A\_LAT} = \begin{bmatrix} -1.0984 & -0.0101 & -0.9999 & 0.3269 & 0.0000 \\ -228.3071 & -0.0012 & 5.2907 & 0.0000 & 0.0000 \\ 26.6357 & -0.1036 & -0.1060 & 0.0000 & 0.0000 \\ 0.0000 & 1.0000 & -0.0101 & 0.0000 & 0.0000 \\ 0.0000 & 0.0000 & 1.0001 & 0.0000 & 0.0000 \end{bmatrix}$$

$$\text{B\_LAT} = \begin{bmatrix} 0.1231 & -0.1515 \\ 796.3443 & 5.9773 \\ -8.3600 & 23.0454 \\ 0.0000 & 0.0000 \\ 0.0000 & 0.0000 \end{bmatrix}$$

< Linear Matrixes, No Damage Condition >

Table 4. Change of the Configuration

Configuration	Damage Condition		Variation Due to Damage (%)
	No Damage	Complex Damage	
Wing Area (m^2)	1.561	1.490	4.5
Wing Span (m)	2.0	1.8	10.0
Mass (kg)	12.003	11.808	1.6
∇CG_x (mm)	0	5.52	- -
∇CG_y (mm)	0	-10.24	- -
∇CG_z (mm)	0	0	- -

$$A\_LON = \begin{bmatrix} -0.3346 & -32.673 & 0.0006 & -9.8057 & 0.0000 \\ -0.0220 & -7.1750 & 0.9487 & 0.0000 & 0.0000 \\ 0.0000 & 34.7158 & -11.0106 & 0.0000 & 0.0000 \\ 0.0000 & 0.0000 & 1.0000 & 0.0000 & 0.0000 \\ 0.0000 & 29.9991 & 0.0000 & -29.9991 & 0.0000 \end{bmatrix}$$

$$B\_LON = \begin{bmatrix} 9.9184 & -2.9781 \\ 0.0031 & -2.2350 \\ 0.0000 & -125.1852 \\ 0.0000 & 0.0000 \\ 0.0000 & 0.0000 \end{bmatrix}$$

$$A\_LAT = \begin{bmatrix} -0.9601 & -0.0093 & -0.9999 & 0.3268 & 0.0000 \\ -208.8113 & -6.2147 & 4.9849 & 0.0000 & 0.0000 \\ 10.6843 & -0.0374 & -0.1224 & 0.0000 & 0.0000 \\ 0.0000 & 1.0000 & -0.0093 & 0.0000 & 0.0000 \\ 0.0000 & 0.0000 & 1.0000 & 0.0000 & 0.0000 \end{bmatrix}$$

$$B\_LAT = \begin{bmatrix} 0.1020 & -0.1227 \\ 560.7239 & 7.1171 \\ -3.9862 & 16.5053 \\ 0.0000 & 0.0000 \\ 0.0000 & 0.0000 \end{bmatrix}$$

< Linear Matrixes, Complex Damage Condition >

3. Reconfigurable Controller Design

3.1 Controller Structure

The overall structure of the reconfigurable controller is described in Fig 5. The outer loop controller was designed to follow the pitch and roll attitude command and the inner loop controller is composed of the baseline body rate controller and the model reference adaptive controller. The inner-loop controllers follow the body rate commands, generated from the attitude errors. The turn coordination algorithm was applied for the yaw axis controller. The model reference adaptive control algorithm maintains or compensates for the performance of the baseline controller even for the complex damage.

3.2 Model Reference Adaptive Control

The reconfigurable flight control system design using the direct model reference adaptive control (MRAC) method was introduced in 2003 [15]. The MRAC method was composed of slow attitude model reference adaptive control loop and fast body rate model reference adaptive control loop. However, it is difficult to design these 2-loop MRAC because the inner-loop and outer-loop reference model must be set under the delicate consideration of the aircraft's flight dynamics as well as the control performance. In this paper, a single loop MRAC was designed in the idea that the performance of the attitude controller is determined by the body rate controller.

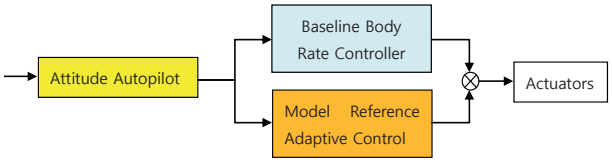

Fig. 5. Reconfigurable Control Structure

The nonlinear aircraft system can be linearized as follows,

$$\dot{x} = Ax + Bu + d$$
$$y = Cx \tag{7}$$

where, $x = [p\ q\ r]'$, $u = [\delta_a\ \delta_e\ \delta_r]'$ and d denotes the disturbances and linearization error. The desired reference model can be set as follows.

$$\dot{y}_m = A_m y_m + B_m r \tag{8}$$

In Eq. (8), A_m is a stable system matrix, B_m is an invertible input matrix, and r is the reference input. As the reference [15], the following controller was applied for MRAC.

$$u = C_0 r + C_0 G_0 x + C_0 \nu\, C_0 K_0 y_m \tag{9}$$

where C_0, G_0 are adaptive gain matrices and ν is an adaptive control vector. Using the above control input, the output error dynamics can be derived as equation (10).

$$\begin{aligned} \dot{e} = \dot{y} - \dot{y}_m &= CAx + CBu + Cd - A_m y_m - B_m r \\ &= (CA + CBC_0 G_0)x + CBC_0 r + CBC_0 \nu \\ &\quad + CBC_0 K_0 y_m + Cd - A_m y_m - B_m r \end{aligned} \tag{10}$$

To make the error converge($\dot{e} \le 0$), following equations should be considered.

$$CA + CBC_0^* G_0^* = A_e C,\ Cd = -CBC_0^* \nu^*,$$
$$B_m = CBC_0^*,\ CBC_0^* K_0^* = A_m - A_e \tag{11}$$

In the equation (11), A_e is an arbitrary stable matrix and the superscript * stands for ideal gain matrices. By substituting the equation (11) into the equation (10), the error equation can be expressed as follows.

$$\begin{aligned} \dot{e} &= (A_e C - CBC_0^* G_0^* + CBC_0 G_0)x + CBC_0 r + CBC_0 \nu \\ &\quad + CBC_0 K_0 y_m - CBC_0^* \nu^* - A_m y_m - CBC_0^* r \\ &= A_e e + (CBC_0 G_0 - CBC_0^* G_0^*)x + CBC_0 r + CBC_0 \nu \\ &\quad + (CBC_0 K_0 - A_m) y_m - CBC_0^* \nu^* - CBC_0^* r + A_e y_m \\ &= A_e e + \{CB(C_0^* + C_0 - C_0^*)G_0 - CBC_0^* G_0^*\}x \\ &\quad + CB(C_0 - C_0^*)r + CBC_0^* \nu + CB(C_0 - C_0^*) \\ &\quad + \{CB(C_0^* + C_0 - C_0^*)K_0 + A_e - A_m\} y_m - CBC_0^* \nu^* \\ &= A_e e + CBC_0^*(G_0 - G_0^*)x \\ &\quad + CB(C_0 - C_0^*)(G_0 x + r + \nu + K_0 y_m) + CBC_0^*(\nu - \nu^*) \\ &\quad + (CBC_0^* K_0 + A_e - A_m) y_m \\ &= A_e e + B_m(G_0 - G_0^*)x \\ &\quad + B_m\left(C_0^{*-1} - C_0^{-1}\right)(C_0 r + C_0 G_0 x + C_0 \nu\, C_0 K_0 y_m) \end{aligned} \tag{12}$$

$$+B_m(\nu - \nu^*)$$

If we define $\Delta G = G_0 - G_0^*, \Delta\Psi = C_0^{*^{-1}} - C_0^{-1}, \Delta\nu = \nu - \nu^*$, and substitute the equation (9) into (12) we can get the following error equation.

$$\dot{e} = A_e e + B_m \Delta Gx + B_m \Delta\Psi u + B_m \Delta\nu \tag{13}$$

From the following Lyapunov candidate function and the Lyapunov stability theorem, the update rules for adaptive gains can be derived.

$$V = e^T P e + \mathrm{tr}\left[\frac{\Delta G^T \Delta G}{\gamma_1}\right] + \mathrm{tr}\left[\frac{\Delta\Psi^T \Delta\Psi}{\gamma_2}\right] + \frac{\Delta\nu^T \Delta\nu}{\gamma_3}$$
$$\text{where, } A_e^T P + P A_e = -Q, \qquad Q > 0. \tag{14}$$

If we define the trim state as the origin, V(0) equals 0 because the error(e), ΔG, $\Delta\Psi$, $\Delta\nu$ are 0 in the trim state. For the all non-zero real vector e, V(e) is positive definite, if we assume that γ_1>0, γ_2>0, γ_3>0. Therefor the equation (14) satisfies the condition of the Lyapunov function.

The time derivative of the equation (14) is as follows.

$$\dot{V} = \dot{e}^T P e + e^T P \dot{e} + 2\mathrm{tr}\left[\frac{\Delta G^T \Delta\dot{G}}{\gamma_1}\right] + 2\mathrm{tr}\left[\frac{\Delta\Psi^T \Delta\dot{\Psi}}{\gamma_2}\right] + \frac{\Delta\nu^T \Delta\dot{\nu}}{\gamma_3} \tag{15}$$

If we apply the error dynamics equation into the equation (15) we can get following equation.

$$\begin{aligned}\dot{V} &= \left(e^T A_e^T + x^T \Delta G^T B_m^T + u^T \Delta\Psi^T B_m^T + \Delta\nu^T B_m^T\right) P e \\ &\quad + e^T P (A_e e + B_m \Delta Gx + B_m \Delta\Psi u + B_m \Delta\nu) \\ &\quad + 2\mathrm{tr}\left[\frac{\Delta G^T \Delta\dot{G}}{\gamma_1}\right] + 2\mathrm{tr}\left[\frac{\Delta\Psi^T \Delta\dot{\Psi}}{\gamma_2}\right] + \frac{\Delta\nu^T \Delta\dot{\nu}}{\gamma_3} \\ &= e^T (A_e^T P + P A_e) e + 2\mathrm{tr}\left[\frac{\Delta G^T}{\gamma_1}\left(\Delta\dot{G} + \gamma_1 B_m^T P e x^T\right)\right] \\ &\quad + 2\mathrm{tr}\left[\frac{\Delta\Psi^T}{\gamma_2}\left(\Delta\dot{\Psi} + \gamma_2 B_m^T P e u^T\right)\right] + \frac{2}{\gamma_3}\Delta\nu^T\left(\Delta\dot{\nu} + \gamma_3 B_m^T P e\right)\end{aligned} \tag{16}$$

To meet the Lyapunov stability condition we can derive the following equations.

$$\Delta\dot{G} = -\gamma_1 B_m^T P e x^T$$
$$\Delta\dot{\Psi} = -\gamma_2 B_m^T P e u^T \tag{17}$$
$$\Delta\dot{\nu} = -\gamma_3 B_m^T P e$$

$$\dot{V} = -e^T Q e \le 0 \tag{18}$$

We can derive the update rules from the equation (17).

$$\dot{G}_0 = -\gamma_1 B_m^T P e x^T \tag{19}$$

$$\dot{C}_0 = -\gamma_2 C_0 B_m^T P e u^T C_0 \tag{20}$$

$$\dot{\nu} = -\gamma_3 B_m^T P e \tag{21}$$

K_0 is derived from the output error dynamics as the following equation.

$$K_0 = B_m^{-1}(A_m - A_e) \tag{22}$$

The derivation of the equations (19) to (22) from the equations (7) to (11) is described in reference [15]. In this paper, the reference model and update rule were designed as follows.

From the equation (8), we set the first order model which has natural frequency of 4rad/sec in roll motion, 3rad/sec in pitch motion and 1rad/sec in yaw motion as the reference model of body rate control as follows.

$$A_m = \begin{bmatrix}-4 & 0 & 0\\ 0 & -3 & 0\\ 0 & 0 & -1\end{bmatrix},\ B_m = \begin{bmatrix}4 & 0 & 0\\ 0 & 3 & 0\\ 0 & 0 & 1\end{bmatrix},$$
$$r = \begin{bmatrix}p_c\\ q_c\\ r_c\end{bmatrix},\ y_m = \begin{bmatrix}p_m\\ q_m\\ r_m\end{bmatrix} \tag{23}$$

For calculation of the gain matrix K_0, Ae matrix was set as following equation (24) to have all negative eigenvalues.

$$A_e = \begin{bmatrix}-2 & 0 & 0\\ 0 & -1.5 & 0\\ 0 & 0 & -1\end{bmatrix} \tag{24}$$

It is very important to set γ because it determines the adaptation rate of the control gains. Therefore it should be designed in the consideration of the aircraft dynamics and actuator performance. In this paper γ was designed as following.

$$\gamma_1 = 0.07,\ \gamma_2 = 0.8,\ \gamma_3 = 0.676 \tag{25}$$

Q matrix was set as $2I_3$, and then P matrix can be calculated from equation (14).

$$P = \begin{bmatrix}0.5 & 0 & 0\\ 0 & 0.667 & 0\\ 0 & 0 & 1\end{bmatrix} \tag{26}$$

3.3 Baseline Body Rate Controller and Attitude Autopilot Design

To meet the requiring control performance with moderate stability margin, the baseline controller should be designed in addition to the MRAC controller. The longitudinal axis

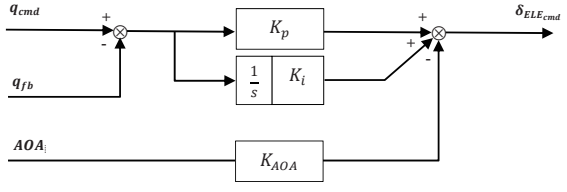

Fig. 6. The longitudinal axis body rate controller

Table 5. Trim State of the Design Point

Trim Condition (Design Point)	Altitude (m)		True Airspeed (m/sec)	
	100		30	
Trim State	Pitch/AOA (deg)	Elevator (deg)	Throttle Level	Aileron/Rudder
	-0.6	-2.5	52.4%	0.0

Table 6. Pole Placement Design of Lateral/Directional Body Rate Controller

	Roll Mode	Spiral Mode	Dutch Roll Mode
Original Poles	-9.46	0.107	-0.179±5.74i
Desired Poles	-4.0	0.1	-1.0, 0.0

Table 7. Feedback Gains

Control Input	K_beta	K_p	K_r	K_phi	K_psi
Aileron	-0.29506	-0.00878	0.00403	0.00018	0.0
Rudder	1.09233	-0.07520	0.12399	-0.01570	0.0

body rate controller structure is shown in Fig. 6.

In this research, the control gains were designed as follows.

$$K_p = 1.125,\ K_i = 0.1125,\ K_{AOA} = 0.1148$$

The lateral-directional axis body rate controller was designed using pole placement method. The design point and trim state are described in Table 5.

The attitude autopilot design is very simple because the autopilot gain can be determined easily from the desired rising time. In this paper, pitch attitude and roll attitude control proportional gains were determined to be 1. Heading controller was designed to calculate the yaw rate command required to coordinated turn from the phi command.

$$r_{cmd} = \frac{g \tan \phi}{2\pi V_t} \tag{27}$$

The velocity hold controller was also designed using a classical PI control structure to maintain the trim velocity during the simulation.

$$K_p = 0.25,\ K_i = 0.06$$

4. Simulation Result

The nonlinear simulation was conducted using MATLAB Simulink software. The Runge-Kutta method was selected as the solver and sampling time was set as 20 msec(50 Hz frame rate). The actuator model was assumed to be the first order lag filter which has a time constant of 0.0625 second. Simulation starts at the wing level trim condition and the

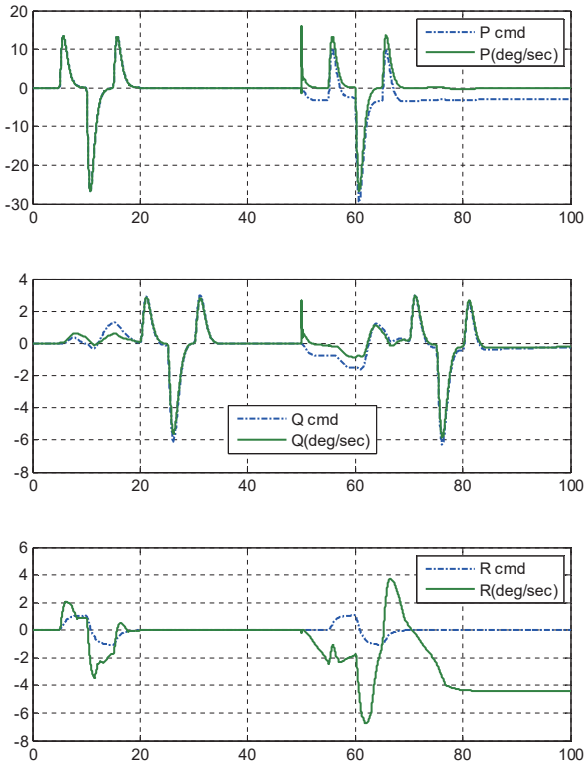

Fig. 7. Body Rate Response(without MRAC), Damage @ 50sec

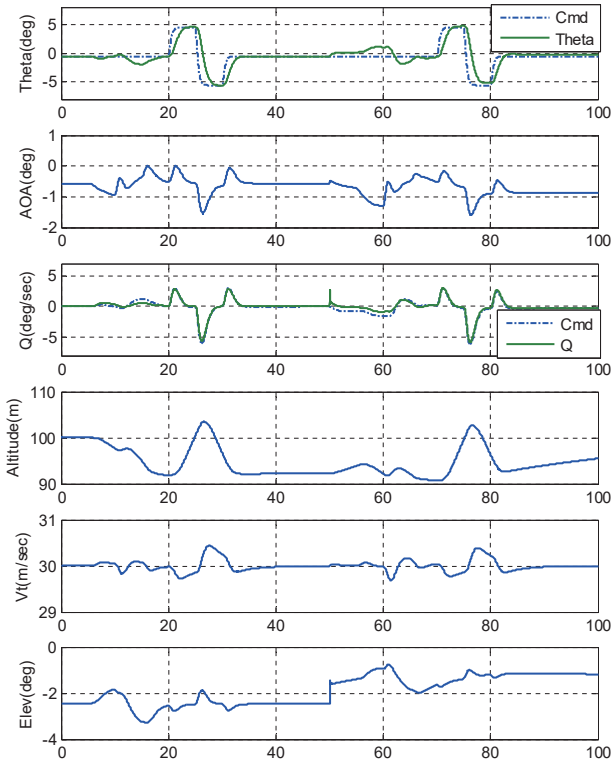

Fig. 8. Longitudinal Response(without MRAC), Damage @ 50sec

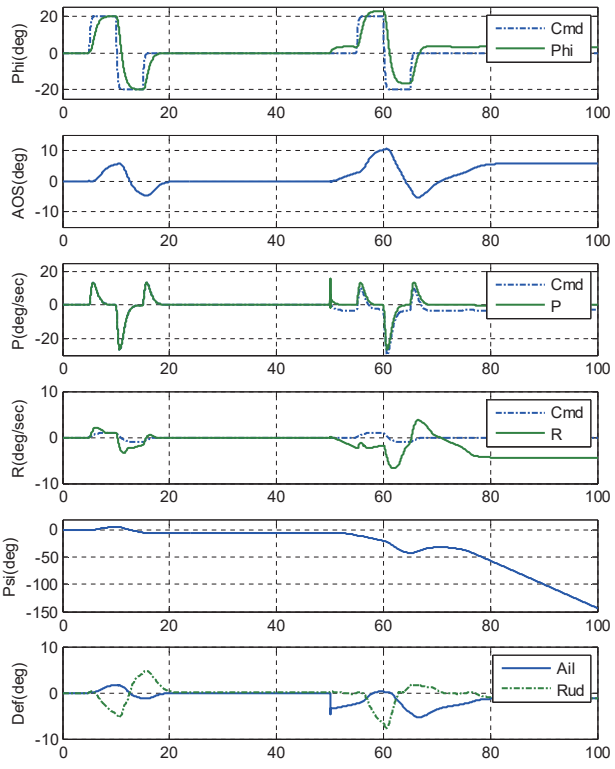

Fig. 9. Lateral-Directional Response(without MRAC), Damage @ 50sec

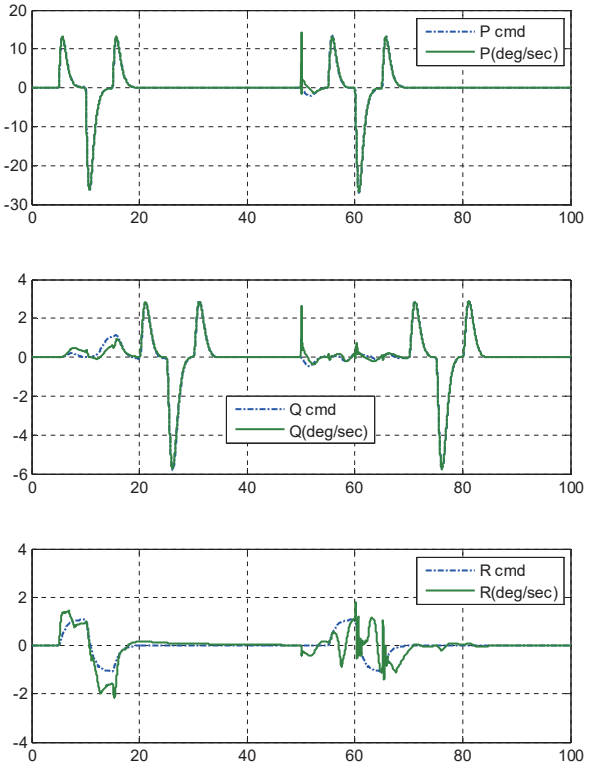

Fig. 10. Body Rate Response(Baseline CLAW + MRAC), Damage @ 50sec

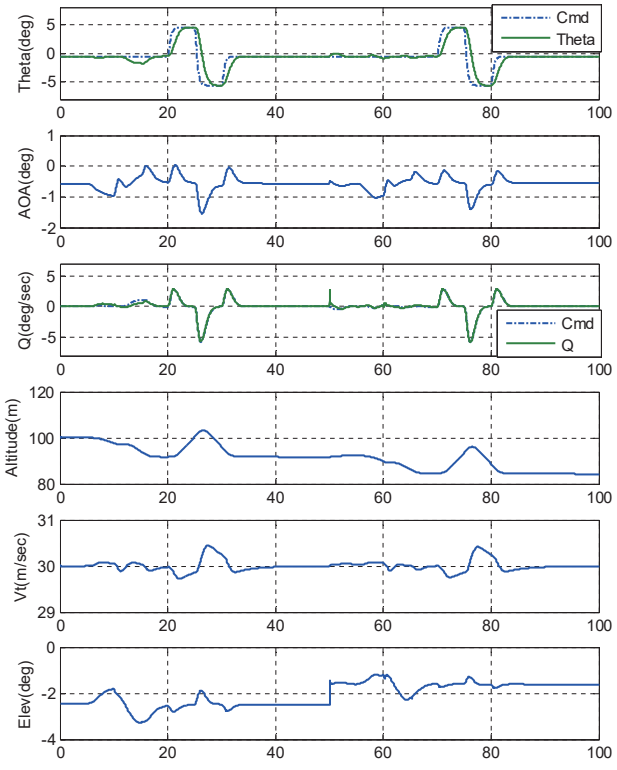

Fig. 11. Longitudinal Response (Baseline CLAW + MRAC), Damage @ 50sec

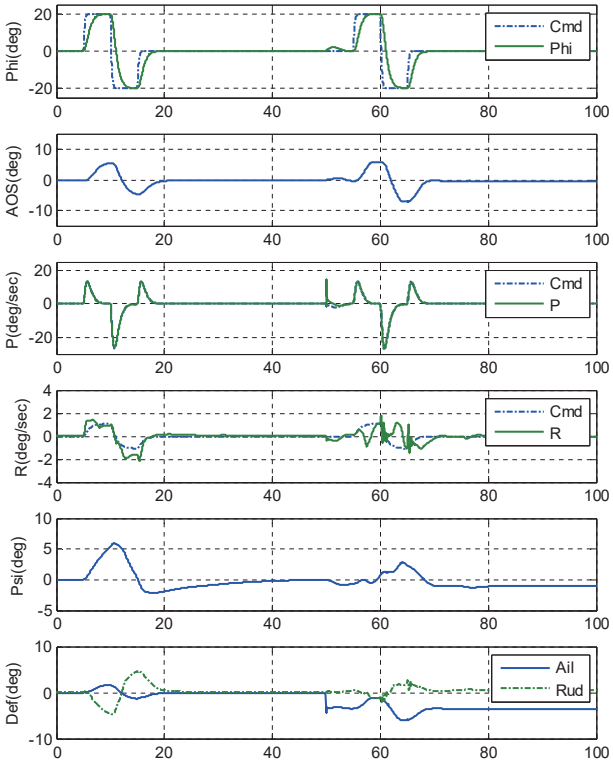

Fig. 12. Lateral-Directional Response (Baseline CLAW + MRAC), Damage @ 50sec

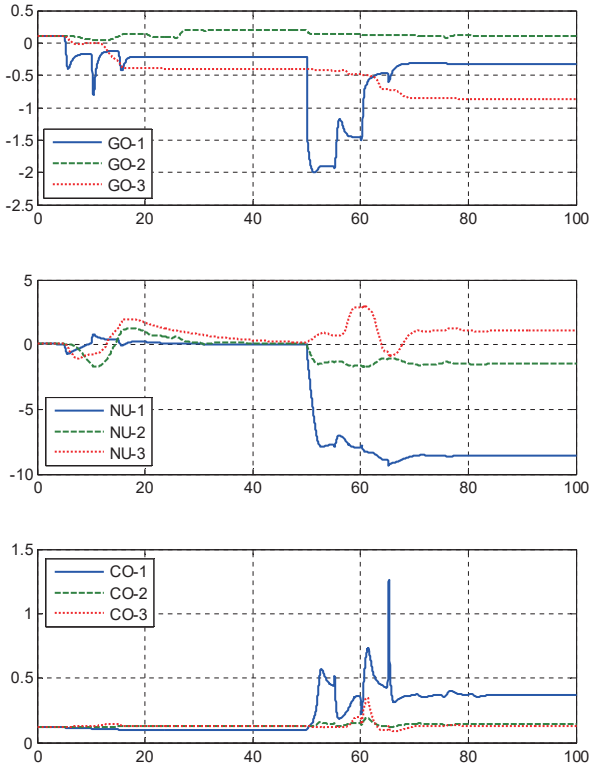

Fig. 13. Adaptive Gains (Baseline CLAW + MRAC), Damage @ 50sec

complex damage is generated after 50second.

Figures 7~9 show the simulation results where the baseline body rate controller and autopilot were activated, without MRAC. In the normal state, the aircraft follows the pitch and roll attitude commands. However, complex damage caused a steady state roll error of 3.4 degrees which the baseline controller could not reduce. Even worse, the degradation of the yaw rate control invoked the heading divergence.

Figures 10~12 show the response of the same simulation scenario but MRAC was activated with the baseline body rate controller. The aircraft follows the pitch and roll attitude commands in the complex damaged state as well as the normal state. Especially, yaw rate control performance was improved to prevent heading divergence and to maintain constant heading after roll out. Fig. 13 shows the variation of the adaptive gains and control vector. In the Fig. 13, C_0 and G_0 are square matrix which have 3 by 3 dimension however only the diagonal terms are indicated on the graph because the cross elements are not dominant in the update of gains. Until 5seconds, all adaptive gains and adaptive control vectors stay initial value, because the error is zero. As the phi command and theta command are applied C_0, G_0 and v start to adapt and converge at 30seconds. After the failure injection the G_0 and v converges to another value to adapt the changed aircraft dynamics. The amount of the variation of the adaptive gains and control vectors became bigger after the complex damage. And it shows that the MRAC worked effectively to minimize the output error.

5. Conclusion

A reconfigurable flight control algorithm that can adapt to complex damage sustained by a BWB aircraft was designed. The direct model reference adaptive controller was designed to restore control performance after taking damage to the UAV's complex damage. The simulation results demonstrated that the designed controller is capable of sustain control performance even after the complex damage correspond to a loss in moment area of 22% and 25% for the right wing and vertical tail(including rudder) respectively. The reconfigurable flight control was conducted only by adapting the inner-loop body-rate controller. If we consider the extended complex damage, we should take into account all control powers, elevators/ailerons/rudder and thrust. The reconfigurable flight control should be extended to flight planning (velocity and path planning) and the autopilot to trim the damaged aircraft. The landing flap configuration also should be considered to adapt the damaged condition. The scope of the future study will cover these issues.

DOI: doi.org/10.5139/IJASS.2017.18.2.290

References

[1] TF-2004-11 DFRC, "Self-Repairing Flight Control System", NASA, Technology Facts.

[2] Kim, B. S. and Calise, A. J., "Nonlinear Flight Control Using Neural Networks", *Journal of Guidance, Control and Dynamics*, Vol. 52, No. 1, 1997, pp. 26-33.

[3] Wise, K. and Brinker, J., "Reconfigurable Flight Control for a Tailless Advanced Fighter Aircraft", *AIAA GNC Conference*, 1998, AIAA 98-4107.

[4] Wise, K., Brinker, J., Calise, A., Enns, D., Elgersma, M. and Voulgaris, P., "Direct Adaptive Reconfigurable Flight Control for a Tailless Advanced Fighter Aircraft", *International Journal of Robust Nonlinear Control*, Vol. 9, 1999, pp. 999-1012.

[5] Calise, A. J., Lee, S. and Sharma, M., "Development of Reconfigurable Flight Control Law for Tailless Aircraft", *Journal of Guidance, Control and Dynamics*, Vol.24, No. 5, 2001, pp. 896-902.

[6] Nguyen, N., Krishnakumar, K., Kaneshige, J. and Nespeca, P. "Dynamics and Adaptive Control for Stability Recovery of Damaged Asymmetric Aircraft", *AIAA Guidance, Navigation, and Control Conference and Exhibit*, Keystone, Colorado, 21 - 24 August 2006.

[7] Jourdan, D., Piedmonte, M., Gavrilets, V., Vos, D., and McCormick, J., "Enhancing UAV Survivability Through Damage Tolerant Control", *AIAA Guidance, Navigation, and Control Conference*, Toronto, Ontario, Canada, 2-5 August 2010, pp. 1-26

[8] Kim, K., Ahn, J. M., Kim, S. K., Kim, D. M., Suk, J., Lim, H., Hur, G. B., Kim, N. and Kim, B. S., "Flight Test of a Flying-Wing Type UAV with Partial Wing Loss Using Neural Network Controller", *AIAA Navigation, and Control Conference*, 2013.

[9] Cao, C. and Hovakimyan, N., "Design and Analysis of a Novel L1 Adatpive Control Architecture, Part I: Control Signal and Asymptotic Stability", *In Proc. of American Control Conference*, 2006, pp. 3397-3402.

[10] Cao, C. and Hovakimyan, N., "Design and Analysis of a Novel L1 Adatpive Control Architecture, Part II: Guaranteed Transient Performance", *In Proc. of American Control Conference*, 2006, pp. 3403-3408.

[11] Cao, C. and Hovakimyan, N., "Novel L1 Neural Network Adaptive Control Architecture with Guaranteed Transient Performance", *IEEE Transactions on Neural Networks*, Vol. 18, No. 4, 2007.

[12] Patel, V. V., Cao, C., Hovakimyan, N., Wise, K. A. and Lavretsky, E., "L1 Adaptive Controller for Tailless Unstable Aircraft", *Proceedings of the 2007 American Control Conference*, Marriott Marquis Hotel at Times Square New York City, USA, July 11-13, 2007.

[13] Kim, K. J., Ahn, J., Kim, S., Choi, J. S., Suk, J., Lim, H. and Hur, G. B., "Analysis of Partial Wing Damage on Flying-wing Unmammed Air Vehicle", *Journal of Aerospace Engineering, Proceedings of the Institution of Mechanical Engineering Part G*, Vol. 228, No. 3, 2014, pp. 355-374.

[14] Ahn, J. M., Kim, K. and Suk, J., "Dynamic Analysis of an Asymmetric UAV with Partial Wing Damage", *International Conference on Control, Automation and Systems(ICCAS)*, October 2011, pp. 112-116.

[15] Kim, K. S., Lee, K. J. and Kim, Y., "Reconfigurable Flight Control System Design Using Direct Adaptive Method", *Journal of Guidance, Control, and Dynamics*, Vol. 26, No. 4, July-August 2003, pp. 543-550.